

## Metal-insulator transition in oxygen-deficient $\text{LaNiO}_{3-x}$ perovskites

R. D. Sánchez,\* M. T. Causa, A. Caneiro, and A. Butera

*Centro Atómico Bariloche and Instituto Balseiro, 8400 San Carlos de Bariloche, Argentina*

M. Vallet-Regí,† M. J. Sayagués,‡ and J. González-Calbet‡

*Instituto de Magnetismo Aplicado, Apartado Postal 155, Las Rozas, E-28230 Madrid, Spain*

F. García-Sanz and J. Rivas

*Departamento de Física Aplicada, Facultad de Física, Universidad de Santiago de Compostela,*

*E-15706 Santiago de Compostela, Spain*

(Received 6 February 1996; revised manuscript received 30 July 1996)

In this work we present a study of the magnetic and transport properties of the system  $\text{LaNiO}_{3-x}$  ( $0 \leq x \leq 0.5$ ) where the  $x=0$  member is a well-known metallic oxide. We found that the  $x=0.5$  compound is an antiferromagnetic insulator at room temperature. The metal-insulator transition is observed for an  $x$  value around  $x \geq 0.25$ . The role played by the sample inhomogeneities on the occurrence of this transition is discussed. [S0163-1829(96)06047-X]

### I. INTRODUCTION

Most of the cations of the first transition row occupying the  $B$  site in oxygen defective  $\text{ABO}_{3-x}$  ( $0 \leq x \leq 0.5$ ) perovskitelike materials have led to the formation of more or less complex superstructures of general formula  $A_n B_n O_{3n-y}$ .<sup>1</sup> The Ni ion is one of the  $B$  cations less studied, mainly due to the difficulty in stabilizing mixed oxides of this element with two different oxidation states. Crespin, Levitz, and Gatineau<sup>2</sup> have successfully isolated the compound  $\text{La}_2\text{Ni}_2\text{O}_5$ , where the oxidation state of Ni is 2+. This compound was obtained from  $\text{LaNiO}_3$  by controlled reduction under a  $\text{H}_2$  atmosphere. These authors also reported the existence of  $\text{LaNiO}_{2.7}$  (with Ni in 2+ and 3+ oxidation states) and  $\text{LaNiO}_2$  (with  $\text{Ni}^{1+}$  only) phases. An electron diffraction study performed by González-Calbet and co-workers<sup>3,4</sup> shows the existence of a homologous series of general formula  $\text{La}_n\text{Ni}_n\text{O}_{3n-1}$ , where the terms  $n=2$  ( $\text{La}_2\text{Ni}_2\text{O}_5$  or  $\text{LaNiO}_{2.5}$ ) and  $n=4$  ( $\text{La}_4\text{Ni}_4\text{O}_{11}$  or  $\text{LaNiO}_{2.75}$ ) are described. The structural model (see Fig. 1) proposed for this homologous series consists of  $n-1$  octahedral layers alternating in an ordered way, with one layer of  $\text{NiO}_4$  square planes along the  $[100]_c$  direction of the perovskite substructure.

Physical properties of the “mother compounds”  $\text{LaNiO}_3$ , which is a well-known metallic oxide, were recently revised by several authors.<sup>5-7</sup> From the observed behavior in specific heat, magnetic susceptibility and electrical resistivity measurements, this compound was described as a correlated electron system with important electron-electron interactions.

Here we present a study of the electrical and magnetic properties of the system  $\text{LaNiO}_{3-x}$ , whose structural properties are similar to those described in Ref. 4. Particularly, we show results for the metal-insulator transition, and the influence of the oxygen vacancy disorder in

this process. The experimental results that we present contribute to studies of local-moments formation starting from a Fermi-liquid system,<sup>8</sup> and also could contribute to a model formulation that includes disorder and interaction effects. These topics have been currently discussed in recent papers.<sup>9</sup>

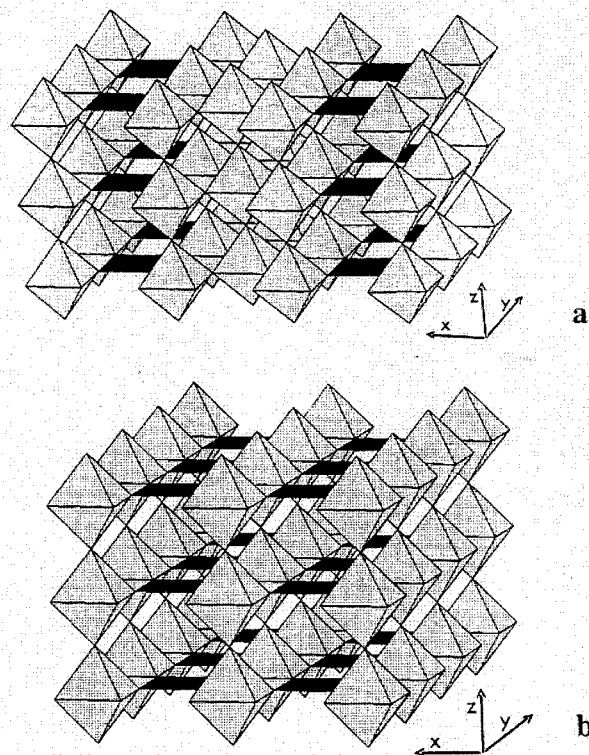


FIG. 1. Structural models proposed in Ref. 4 for (a)  $\text{LaNiO}_{2.75}$  and (b)  $\text{LaNiO}_{2.50}$ . The unoccupied oxygen position yields square planar coordination for Ni ions.

## II. EXPERIMENT

LaNiO<sub>3</sub> was prepared by a liquid mix technique as described in Refs. 3 and 6. The sample obtained shows a rhombohedral unit cell that, indexed in a hexagonal cell, has lattice parameters of  $a=5.456(1)$  Å and  $c=13.136(2)$  Å. LaNiO<sub>3-x</sub> was obtained from LaNiO<sub>3</sub> by using a symmetrical thermobalance based on a Cahn 1000 electrobalance. The experimental details and performance of this equipment were described in Ref. 10. The partial oxygen pressure of the gaseous atmosphere was continuously monitored by means of a zirconia oxygen sensor, and the gas flow rates were controlled through mass flow controllers.

LaNiO<sub>2.75</sub> and LaNiO<sub>2.50</sub> were prepared<sup>4</sup> by reduction under a flowing H<sub>2</sub>/Ar mixture at a constant temperature as follows. A sintered sample of about 1 g of LaNiO<sub>3</sub> was heated at 500 °C under 1 atm of pure O<sub>2</sub> for 2 h. This procedure eliminates any volatile products absorbed on the sample. Then the temperature was decreased to 300 °C, and the O<sub>2</sub> atmosphere was purged with pure Ar. H<sub>2</sub> was subsequently mixed with the Ar in a H<sub>2</sub>/Ar ratio of 0.2. In this condition the reduction process begins. The H<sub>2</sub> flow was interrupted when the weight loss ended. Finally, the temperature was raised to 400 °C over 8 h to improve the homogeneity. During this procedure no weight change was observed.

The samples were also studied before the last step of annealing. As we will see below in the case when  $x=0.25$ , differences were found between 400 °C thermally treated samples LaNiO<sub>2.75</sub>, and the thermally treated samples LaNiO<sub>2.75ξ</sub>.

All the samples, controlled by x-ray diffractometry, were single phase. The electron-diffraction characterization shows that samples with  $x=0.5$  and  $0.25$  in LaNiO<sub>3-x</sub> correspond to the  $n=2$  and members, respectively, of the homologous series La<sub>*n*</sub>Ni<sub>*n*</sub>O<sub>3*n*-1</sub> (see Fig. 1).

The electrical conductivity was measured by a standard dc four-probe method in the temperature range 10–300 K. The resistance  $R$  shows variations of several orders of magnitude depending on samples and temperatures. In order to improve the experimental accuracy, the measurements were performed with a constant electrical current intensity covering the range from  $\mu$ A to mA.

The susceptibility was measured with a superconduction quantum interference device magnetometer [for  $5 \leq T(K) \leq 300$ ], with a Faraday magnetometer [for  $50 \leq T(K) \leq 300$ ], and with a vibrating sample magnetometer in the range 300–700 K. The dependence  $M$  vs  $H$  in the reduced samples ( $x>0$ ) was linear only for  $H>1$  kG, and could be described by  $M=M_0+\chi H$ .  $M_0$  was sample dependent, reaching random maximum values ( $\leq 57$  emu/mole) at  $T\sim 280$  K. In all the cases  $M_0$  vanishes for  $T>620$  K. We associate this remanent magnetization with small amounts of metallic Ni coming from the reduction process.<sup>11</sup> Therefore the true susceptibility of LaNiO<sub>3-x</sub> is the high-field susceptibility  $\chi$ .

### A. Results

#### 1. Electrical conductivity

In Fig. 2, the  $T$  dependence of the electrical resistivity is shown for all the studied samples  $x=0, 0.25, 0.25\xi$ , and  $0.5$ .

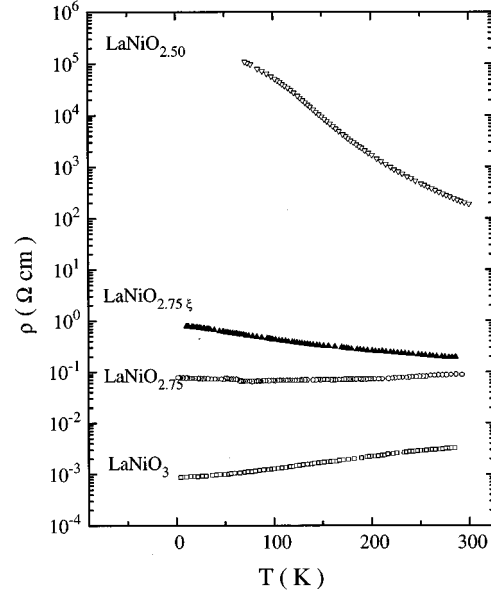


FIG. 2. Electrical resistivity ( $\rho$ ) vs  $T$  for LaNiO<sub>3-x</sub> with  $x=0, 0.25, 0.25\xi$ , and  $0.5$  oxygen compositions. The metal-insulator transition occurs at  $x\geq 0.25$ . The sample obtained before the last step of annealing at 400 °C is labeled with  $\xi$ .

At high temperatures a metal-insulator transition as a function of  $x$ , suggested for the change in the sign of  $\partial\rho/\partial T$ , can be seen for  $x\approx 0.25$ .

Notice the differences between the two  $x=0.25$  samples. A plot of the electrical conductivity for these samples is presented in Fig. 3. In the case of a 400 °C thermally annealed sample (LaNiO<sub>2.75</sub>), a change in the sign of  $\partial\sigma/\partial T$  at  $T\sim 75$  K is observed, being  $\partial\sigma/\partial T>0$  at  $T<75$  K. For higher  $T$ ,  $\partial\sigma/\partial T<0$ , and a linear behavior for  $\sigma$  vs  $T$  is

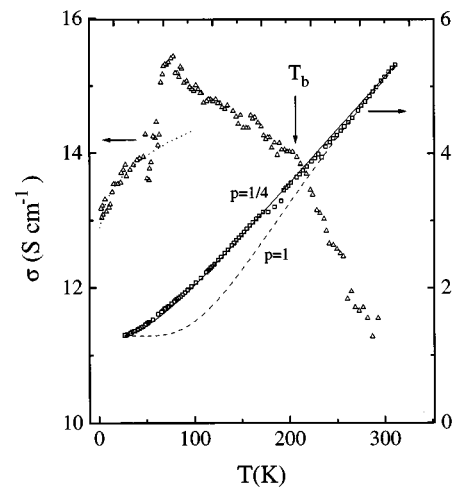


FIG. 3. Details of the metal-insulator transition. The electrical conductivity ( $\sigma$ ) of LaNiO<sub>2.75ξ</sub> ( $\square$ ) is shown in the right axis. The solid line represents the best fit to Eq. (2.2), with  $p=1/4$  and the dashed line with  $p=1$ . In both cases the same metallic contribution  $\sigma_{0M}/(1+aT)$  was added. The left axis shows  $\sigma$  of LaNiO<sub>2.75</sub> ( $\triangle$ ), which has been fitted by  $\sigma=\sigma_0+\alpha T^{1/3}$  (dotted line) at  $T<75$  K. A change of slope is observed at 220 K in coincidence with the  $T_b$  observed in  $\chi$ .

found with a change in the slope value at  $T \sim 220$  K. In the metal-insulator transition region, for  $T \leq 75$  K,  $\sigma(\text{LaNiO}_{2.75})$  was fitted<sup>12</sup> by  $\sigma = \sigma_0 + \alpha T^{1/3}$ , with  $\sigma_0 = 12.5$  (0.1)  $\text{S cm}^{-1}$  and  $\alpha = 0.40$  (0.03)  $\text{S cm}^{-1} \text{K}^{-1/3}$ , as is shown in Fig. 3.

The unannealed sample  $\text{LaNiO}_{2.75\xi}$  shows a lower conductivity and no change in the sign of  $\partial\sigma/\partial T$  was observed for  $10 \leq T(\text{K}) \leq 300$ . The differences found in the electrical properties between the two  $x=0.25$  samples cannot be attributed to the oxygen content, which was constant during the 400 °C annealing process. In Ref. 4 an electron-diffraction study of 400 °C annealed samples is reported. The observed superstructures were interpreted considering O-vacancy long-range ordering as shown in Fig. 1(a). Our results, obtained repeatedly on samples of different bulks, indicate that without the last step of annealing the O-vacancy ordering is not well established along the sample volume. Then the observed lowering in the conductivity (see Fig. 2) could be associated with the lattice disorder.

For samples which show semiconducting behavior for all  $T$ ,  $\sigma$  can be approximated for the general relationship

$$\sigma = A \exp(-B/T^p). \quad (2.1)$$

The exponent  $p$  can take some defined values, depending on the operating electrical transport mechanism. If  $p=1$  the  $B$  parameter gives an estimation of the energy gap ( $E_a/k_B$ ) between the conduction and valence bands. From a  $\ln\sigma$  vs  $T^{-1}$  plot in the 210–300-K temperature range, we obtained  $E_a = 0.12$  and 0.03 eV for  $\text{LaNiO}_{2.50}$  and  $\text{LaNiO}_{2.75\xi}$ , respectively.

Below 210 K, for the  $x=0.25\xi$  sample, deviations from this semiconducting behavior are observed (see Fig. 3) which can be explained by a  $T$ -dependent activation energy. In an Anderson band picture two mobility edges ( $E_c$  and  $E'_c$ ) exist, which separate localized (in the band tails) from nonlocalized states (between the energy edges). The localized states are a consequence of a random potential or disorder present in the system. For the cases where the Fermi energy  $E_F < E_c$ , two conduction mechanisms can be present: (a) *Excitation of the carrier to a mobility edge*. In this case  $\sigma$  can be described by Eq. (2.1) with  $p=1$  and  $B = (E_c - E_F)/k_B$ ; these electrons, localized in the band tails, need higher thermal energies or a  $E_F$  near  $E_c$ . (b) *Thermally activated hopping*. In this case, at liquid-helium temperature, the electron hopping between localized states can be observed. For this mechanism called variable range hopping (VRH) (Ref. 13) for a three dimensional system, is  $p \approx \frac{1}{4}$  and  $B = T_0^{1/4}$  in Eq. (2.1) (Mott's formula). In some cases, a VRH dependence is observed at high temperatures, above half the Debye temperature [ $T \geq (\Theta_D/2)$ ], and explained by polaron hopping.<sup>14</sup>  $\text{LaNiO}_{2.75\xi}$  could be described by a VRH model in the 120–300-K range. However, our experimental data do not extrapolate to null conductivity in the  $T \rightarrow 0$  limit. In order to fit the conductivity of  $\text{LaNiO}_{2.75\xi}$  in all experimental  $T$  ranges, an extra conductivity channel with metallic behavior is added to Eq. (2.1):

$$\sigma = \frac{\sigma_{0M}}{1+aT} + A \exp(-B/T^p), \quad (2.2)$$

TABLE I. Fitted values obtained with a function  $\sigma = A \exp(-B/T^p)$  from the semiconductinglike experimental data. The symbol  $\xi$  indicates the unannealed samples; data with  $p=1$  and  $\frac{1}{4}$  are shown by dashed and solid lines, respectively in Fig. 3.  $\Delta\sigma$  is the difference between  $\sigma_{\text{expt.}}$  and  $\sigma_{\text{fit}}$ .

Sample	A ( $\text{S cm}^{-1}$ )	B ( $\text{K}^p$ )	$p$	T range (K)	$(\Delta\sigma)/\sigma$ (%)
$\text{LaNiO}_{2.75\xi}$	381(200)	18.7(0.7)	$\frac{1}{4}$	300-10	$\leq 3$
	12.8(0.1)	332(3)	1	300-210	$\leq 3$
$\text{LaNiO}_{2.50}$	$56(2) \times 10^{-2}$	1400(10)	1	300-210	$\leq 9$

where  $\sigma_{0M} = 1.28(0.02)$   $\text{S cm}^{-1}$  and  $a = 1.5 \times 10^{-5}$   $\text{K}^{-1}$  were obtained from the fitting procedure. Due to the small value of  $a$ , the first term in Eq. (2.2) is approximately constant with  $T$ , the second term was already discussed. Equation (2.2) has the same form as the conductance ( $G$ ) of an inhomogeneous media just above the percolation threshold of the conductor, where  $G = F_1\sigma_1 + F_2\sigma_2$ , with  $\sigma_1 \gg \sigma_2$ .<sup>15</sup> Two similar phenomenological channel models were proposed in order to explain the electrical behavior of inhomogeneous  $\text{La}_{0.66}\text{Ca}_{0.33}\text{MnO}_3$  (Ref. 16) and granular Al (metallic) in  $\text{Al}_2\text{O}_3$ .<sup>17</sup> In Table I we summarize the results of the different fitting procedures for the different samples studied.

## 2. Magnetic susceptibility

The  $\chi$  vs  $T$  dependence for  $x=0$  and 0.25 is shown in Fig. 4(a), measured with an external magnetic field  $H=5$  kG.

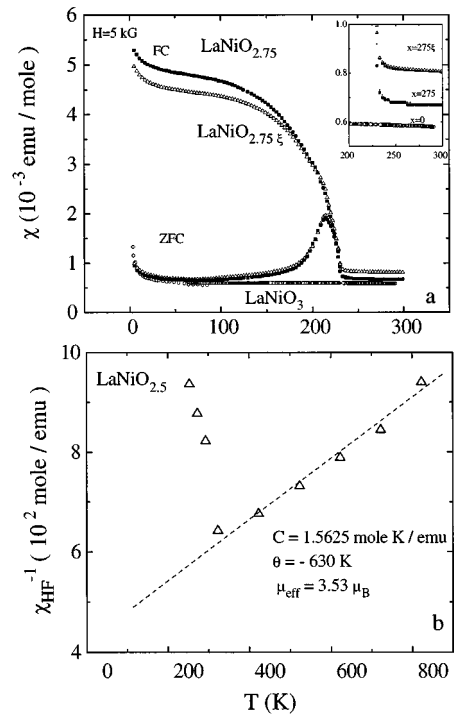


FIG. 4. Magnetic susceptibility ( $\chi$ ) vs  $T$  (a) for  $x=0$ , 0.25, and 0.25 $\xi$ . The enhancement of the Pauli contribution to  $\chi$  is shown in the inset. For  $x=0.25$  and 0.25 $\xi$ , the differences between FC (field cooling) and ZFC (zero-field cooling) were observed for  $T < T_b = 220$  K. (b)  $\chi$  for  $x=0.5$  suggests antiferromagnetic order below room temperature.

The  $T$  dependence, for  $x=0$ , can be described by  $\chi = \chi_{\text{Pauli}} + C/T$ , with  $\chi_{\text{Pauli}} = 5.6 \times 10^{-4}$  emu/mole and  $C = 1 \times 10^{-3}$  emu K/mole. For  $x=0.25$ , ZFC (zero field-cooling) and FC (field cooling) experiments give different values of  $\chi$  below a characteristic temperature ( $T_b = 220$  K). These results indicate spin localization and magnetic order frustration. Similar  $\chi$  vs  $T$  dependences are usually observed in other systems such as spin-glass-like compounds (where  $T_b$  would be the freezing temperature) or magnetic fine particles (where  $T_b$  would be the blocking temperature). Actually, susceptibility measurements on  $\text{LaNiO}_{2.70}$  showing similar behavior were analyzed<sup>23</sup> in terms of ferromagnetic clusters of different sizes. Nevertheless the origin of these clusters remains uncertain.<sup>23</sup> At  $T > T_b$ , enhancements of  $\chi_{\text{Pauli}}$  were observed in coincidence with increasing  $\rho$  [see the inset of Fig. 4(a)]. This enhancement in  $\chi$  near a metal-insulator transition is explained by an increase in the effective mass ( $\chi \propto m^*/m$ ) expected in a Fermi-liquid model.<sup>18</sup> No differences between  $T_b$  of  $\text{LaNiO}_{2.75\xi}$  and  $\text{LaNiO}_{2.75}$  have been observed. However, at higher temperature ( $T > 330$  K), while an independent  $T$  value  $\chi$  in  $\text{LaNiO}_{2.75}$  was observed,  $\text{LaNiO}_{2.75\xi}$  showed a clear Curie-Weiss behavior with a negative Curie-Weiss temperature  $\Theta \cong 45$  K. From the Curie constant we obtain the effective number of Bohr magnetons  $\mu_{\text{eff}} = 1.86$ .

For the  $x=0.5$  sample,  $\chi$  vs  $T$  is shown in Fig. 4(b). We found a broad peak at  $T_N = 320$  K and a Curie-Weiss behavior at high temperatures with a negative Curie-Weiss temperature  $\Theta \cong 630$  K that shows strong antiferromagnetic interactions. From the Curie constant we obtain  $\mu_{\text{eff}} = 3.5\mu_B$ , which is near the expected value for  $\text{Ni}^{2+}$  ( $S=1$  and  $g \sim 2.3$ ). The ratio  $\Theta/T_N \cong 2$  suggests some degree of frustration in the magnetic system.

### III. DISCUSSION

The reduction of  $\text{LaNiO}_3$  changes the valence state and O coordination of Ni ions. These changes must modify the band structure of the different compounds of the  $\text{LaNiO}_{3-x}$  series. As  $\text{LaNiO}_3$  is a charge-transfer metal,<sup>19</sup> the conductivity properties of  $\text{LaNiO}_{3-x}$  should be determined by the interplay between the bandwidth and energy gaps of the O and Ni bands, as sketched in Fig. 5. For  $\text{LaNiO}_3$ ,  $\Delta \ll U_{\text{eff}}$ , where  $\Delta$  is the gap between  $2p$ -O and  $3d^8$ -Ni bands, and  $U_{\text{eff}}$  is the gap between the Ni bands  $3d^8$  and  $3d^7$ .<sup>20,21</sup> On the other side, for  $\text{LaNiO}_{2.5}$ ,  $U_{\text{eff}} \ll \Delta$ , and the Fermi level should be between the  $3d^9$  and  $3d^8$  bands (see Fig. 5). Similar to NiO or  $\text{La}_2\text{NiO}_4$ ,<sup>21</sup>  $\text{LaNiO}_{2.50}$  is an insulator and antiferromagnetic. On going from  $\text{LaNiO}_3$  to  $\text{LaNiO}_{2.5}$ , an enlargement of the cell volume is observed,<sup>2</sup> attributed to the increase in the average ionic radius of Ni ( $r=0.60$  for  $\text{Ni}^{3+}$  and  $r=0.69$  for  $\text{Ni}^{2+}$ ). As the Ni-O distance increases, the electronic transfer parameter  $t$  and the bandwidth ( $W \propto t$ ) diminish. Electron localization then takes place. The localization may also be favored for a decreasing state density as a consequence of the O vacancies produced in the neighborhood of the Ni ions. In the reduced samples these are two different sites for the  $\text{Ni}^{2+}$  ion: sites with six oxygen ion nearest neighbors in an octahedral ( $O_h$ ) symmetry, and sites with four oxygen nearest neighbors in a squared plane ( $D_{4h}$ ) symmetry. The electronic band with  $e_g$  character

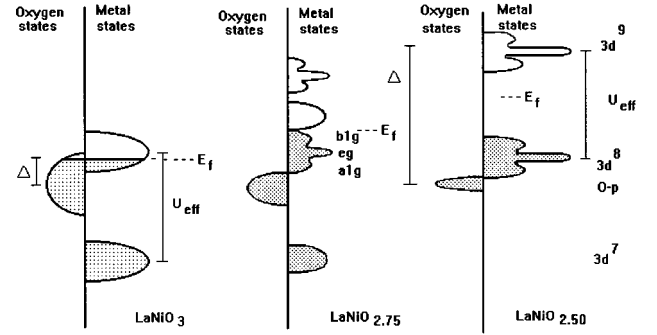


FIG. 5. Band scheme proposed in order to explain the behavior observed in  $\text{LaNiO}_{3-x}$ . On the left side we show the  $\text{LaNiO}_3$  case, where the overlapped  $\text{Ni}^{3+}$  and  $\text{O}^{2-}$  bands give the metallic behavior. On the right side the  $\text{LaNiO}_{2.5}$  case is seen, which has insulator electrical properties and two different  $\text{Ni}^{2+}$  symmetries.  $\text{LaNiO}_{2.75}$ , in the middle, is presented with a small gap. Increasing  $x$  (or from left to right) we can see a progressive narrowing band due to the localization. For the O band the narrowing is more important because the reduction process diminishes the number of states. The shadow region shows the occupied band states.

splits into  $a_{1g}$  and  $b_{1g}$  bands for octahedral and squared plane environments, respectively.

In the  $x=0.25$  sample, where the oxygen vacancies are ordered, a sign change of  $d\sigma/dT$  occurs at 75 K, which could be explained by a  $T$ -dependent bandwidth  $W(T)$ . The electrical conductivity can be described by a power law ( $\sigma = \sigma_0 + aT^{1/3}$ ) below 75 K. Above 75 K a metallic  $\sigma$  is observed with a slope change at 220 K, coincident with  $T_b$ , the characteristic temperature where some degree of magnetic ordering seems to be present. This behavior can be compared with changes in the conductivity observed in ferromagnetic metal oxides because of the electron-magnon scattering.<sup>22</sup>

Finally, we find that the absence of the last step of annealing at 400 °C modifies the magnetic and electrical conductivity properties of the  $x=0.25$  samples. In  $\text{LaNiO}_{2.75\xi}$  we have observed the following: (i) a Curie-Weiss  $T$  dependence of  $\chi$  at higher temperatures, (ii) a sign change of  $d\sigma/dT$ , (iii) a diminishing in the conductivity for all temperatures, and (iv) in all the experimental  $T$  range,  $\sigma(x=0.25\xi$  and  $T)$  can be described with a two-channel model: metallic plus VRH mechanisms. These two parallel electrical resistivity channels can originate in the inhomogeneities of the unannealed sample. This behavior is interpreted as the presence of threads or islands in metallic contact, rich in oxygen, imbedded in an insulator medium rich in oxygen vacancies. It is noticeable the  $p \approx \frac{1}{4}$  in the second term of Eq. (2.2) may be indicating the presence of localized states for which  $\sigma$  is described by Mott's formula. A poor conductivity is expected if the system has an oxygen vacancy disorder, and would present a lower  $\sigma$  than the case with an oxygen vacancy order. Further studies of the enhancement of the specific-heat coefficient  $\gamma$  in  $\text{LaNiO}_{3-x}$ , with  $x=0.25$  and 0.5, are necessary for a full theoretical description of the system.

### ACKNOWLEDGMENTS

We acknowledge partial support from the Ministerio de Educación y Ciencia de España through the Programa de

Cooperación Científica con Iberoamérica, and from the Consejo Nacional de Investigaciones Científicas y Técnicas de Argentina through the PID 304370085. Financial support from CICYT (Spain) (Project

Nos. MAT91-0331, MAT 93-0207, and PB94-1528), and from the Commission of the European Communities DG XII-G (Contract No. CII\*CT92-0087) are also acknowledged.

\*Present address: Dept. Física Aplicada, Fac. de Física, Univ. de Santiago de Compostela, E-15706 Santiago de Compostela, Spain.

†Also at Departamento de Química Inorgánica y Bioquímica, Facultad de Farmacia, Universidad Complutense, E-28040 Madrid, Spain.

‡Also at Departamento de Química Inorgánica y Bioquímica, Facultad de Química, Universidad Complutense, E-28040 Madrid, Spain.

<sup>1</sup>M. T. Anderson, J. T. Vanghey, and K. R. Poeppelmeier, *Chem. Mater.* **5**, 151 (1993); A. Reller, D. A. Jefferson, J. M. Thomas, and M. K. Uppal, *Proc. R. Soc. London Ser. A* **394**, 223 (1984); J. M. González-Calbet, M. Parras, J. Alonso, and M. Vallet-Regí, *J. Solid State Chem.* **111**, 202 (1994).

<sup>2</sup>M. Crespín, P. Levitz, and L. Gatineau, *J. Chem. Soc. Faraday Trans.* **79**, 1181 (1983).

<sup>3</sup>J. M. González-Calbet, M. J. Sayagués, and M. Vallet-Regí, *Solid State Ionics* **32/33**, 721 (1989).

<sup>4</sup>M. J. Sayagués, M. Vallet-Regí, A. Caneiro, and J. M. González-Calbet, *J. Solid State Chem.* **110**, 295 (1994).

<sup>5</sup>A. K. Raychaudhuri, K. P. Rajeev, H. Srikanth, and R. Mahendiran, *Physica B* **197**, 124 (1994).

<sup>6</sup>R. D. Sánchez, M. T. Causa, M. J. Sayagués, M. Vallet-Regí, and J. M. González-Calbet, *J. Alloy. Compd.* **191**, 287 (1993); R. D. Sánchez, Ph.D. thesis, Instituto Balseiro Argentina, 1992.

<sup>7</sup>K. Sreedhar, J. M. Honing, M. Darwin, M. McElfresh, P. M. Shand, J. Xu, B. C. Crooker, and J. Spalek, *Phys. Rev. B* **46**, 6382 (1992).

<sup>8</sup>M. Milovanović, S. Sachdev, and R. N. Bhatt, *Phys. Rev. Lett.* **63**, 82 (1989); S. Sachdev, *Phys. Rev. B* **39**, 5297 (1989).

<sup>9</sup>M. A. Tush and D. E. Logan, *Phys. Rev. B* **51**, 11 940 (1995); **48**, 14 843 (1993).

<sup>10</sup>A. Caneiro, Ph.D. thesis, Instituto Balseiro Argentina, 1983.

<sup>11</sup>J. M. González-Calbet, M. Vallet-Regí, M. J. Sayagués, R. D. Sánchez, and M. T. Causa, *J. Mater. Res.* **9**, 176 (1994).

<sup>12</sup>D. J. Newsom and M. Pepper, *J. Phys. C* **19**, 3983 (1986); H. C. Malieppaard, M. Pepper, R. Newbury, and G. Hill, *Phys. Rev. Lett.* **61**, 367 (1987); A. K. Raychaudhuri, K. P. Rajeev, H. Srikanth, and R. Mahendiran, *Physica B* **197**, 124 (1994).

<sup>13</sup>N. F. Mott, *Metal Insulator Transition*, 2nd ed. (Taylor and Francis, London, 1991); N. F. Mott and E. A. Davis, *Electronic Processes in Non-Crystalline Materials* (Clarendon, Oxford, 1979).

<sup>14</sup>D. Emin, *Phys. Rev. Lett.* **32**, 303 (1974); *Adv. Phys.* **24**, 305 (1975).

<sup>15</sup>D. J. Bergman and D. Stroud, in *Solid State Physics*, edited by H. Ehrenreich and D. Turnbull (Academic, New York, 1992), Vol. 46, p. 147.

<sup>16</sup>J. E. Nuñez-Regueiro and A. M. Kadin, *Appl. Phys. Lett.* **68**, 2747 (1996).

<sup>17</sup>W. L. McLean, P. Lindenfeld, and T. Worthington, in *Electrical Transport and Optical Properties of Inhomogeneous Media, Ohio, 1977*, edited by J. C. Garland and D. B. Tanner, AIP Conf. Proc. No. 40 (American Institute of Physics, New York, 1978), pp. 403–407.

<sup>18</sup>J. Spalek, *J. Solid State Chem.* **88**, 70 (1990).

<sup>19</sup>J. B. Torrance, P. Lacorre, A. I. Nazal, E. J. Ansaldo, and Ch. Niedermayer, *Phys. Rev. B* **45**, 8209 (1992).

<sup>20</sup>J. Zaanen, G. A. Sawatzky, and J. W. Allen, *Phys. Rev. Lett.* **55**, 418 (1985).

<sup>21</sup>J. Torrance, P. Lacorre, Ch. Asavaroengchai, and R. Metzger, *Physica C* **182**, 352 (1991).

<sup>22</sup>W. H. Kettler and M. Rosenberg, *Phys. Rev. B* **39**, 12 142 (1989).

<sup>23</sup>Y. Okajima, K. Kohn, and K. Siratori, *J. Magn. Magn. Mater.* **140-144**, 2149 (1995).